The synthesis, characterization and optical properties of novel 2-acyl 6-arylindolizines

Yan Qing Ge, Xue Yong Gong, Guang Jie Song, Xiao Qun Cao, Jian Wu Wang

PII: S1386-1425(14)01045-2
DOI: http://dx.doi.org/10.1016/j.saa.2014.06.146
Reference: SAA 12405

To appear in: *Spectrochimica Acta Part A: Molecular and Biomolecular Spectroscopy*

Received Date: 7 April 2014
Revised Date: 6 June 2014
Accepted Date: 29 June 2014

Please cite this article as: Y.Q. Ge, X.Y. Gong, G.J. Song, X.Q. Cao, J.W. Wang, The synthesis, characterization and optical properties of novel 2-acyl 6-arylindolizines, *Spectrochimica Acta Part A: Molecular and Biomolecular Spectroscopy* (2014), doi: http://dx.doi.org/10.1016/j.saa.2014.06.146

The synthesis, characterization and optical properties of novel 2-acyl 6-arylindolizines

Yan Qing Ge[a], Xue Yong Gong[a], Guang Jie Song[a], Xiao Qun Cao[a*], Jian Wu Wang [b*]

[a]School of Chemical Engineering, Taishan Medical University, Taian, Shandong, 271016, PR China.

[b]School of Chemistry and Chemical Engineering, Shandong University, Jinan, Shandong, 250100, PR China.

[*]Corresponding author. Tel.: +86 538 6236195, fax: +86 538 6229741,

E-mail: xqcao@tsmc.edu.cn(Xiao Qun Cao); jwwang@sdu.edu.cn(Jian Wu Wang).

Abstract

A series of novel 2-acyl-6-aryl substituted indolizine derivatives was synthesized by a novel tandem reaction between 4-acyl-pyrrole-2-carbaldehyde derivatives and ethyl 4-bromo-3-arylbut-2-enoate under mild conditions. The compounds were characterised using IR, ^{1}H NMR ^{13}C NMR and HRMS. The crystal structure of **7a** was determined using single crystal X-ray crystallography. The absorption results showed that compounds **7a-e** presented their absorption maxima at ca. 270 nm, while compounds **7f** and **7g** with a larger conjugation system exhibited red-shifted absorption character (ca. 280 nm). Fluorescence spectra revealed that these compounds exhibited blue fluorescence (434-456 nm) in dilute solutions and showed quantum yields of fluorescence between 0.02 and 0.39 in dichloromethane.

Key words: Synthesis, Tandem, Indolizine, Nitrogen-bridgehead, UV absorption, Fluorescence

1. Introduction

Nitrogen-bridgehead heterocycles have attracted considerable attention from medicinal and organic chemists due to their wide variety of biological activities and optical/electrical properties, and many of attractive methods have been developed for synthesizing this class of compounds. Of these heterocycles, indolizines play important roles as calcium entry blockers[1], potential central nervous system depressants[2], 5-HT3 receptor antagonist[3], histamine H3 receptor antagonists[4], cardiovascular agents[5], and PLA2 inhibitors[6].

The indolizine ring has a large dipole moment due to the non-uniform charge

distribution in the five-membered and six-membered rings (Fig. 1). Within the indolizine ring, electronic charge builds up significantly in the five-membered ring while low electron density appears in the six-membered ring. Conjugated organic compounds with large polarizabilities are of particular use in the field of optical electronics, such as non-linear optics [7]. To date little attention has been paid to the photophysical properties of these indolizine derivatives[8-12]. Continuing our efforts on extending the scope and applications of the tandem reaction for the preparation of nitrogen-bridgehead heteroaromatics [13-15] and in order to search for novel fluorescent organic compounds with potential bioactivities[16-22], herein, 2-acyl-6-arylindolizines were conveniently synthesized by a novel tandem reaction under mild conditions and their structure and optical properties were described.

Fig. 1

2. Experimental

2.1. General

All reagents were commercially available and used without further purification. Melting points were determined on an XD-4 digital micro melting point apparatus. ^{1}H NMR spectra were recorded on a Bruker Avance 300 (300 MHz) spectrometer, using $CDCl_3$ as solvent and tetramethylsilane (TMS) as internal standard. IR spectra were recorded with an IR spectrophotometer VERTEX 70 FT-IR (Bruker Optics). HRMS spectra were recorded on a Q-TOF6510 spectrograph (Agilent). UV-vis spectra were recorded on a U-4100 (Hitachi). Fluorescent measurements were recorded on a Perkin-Elmer LS-55 luminescence spectrophotometer.

2.2. Synthesis

*2.2.1 General procedure for the preparation of **3***

As shown in Fig. 2, compounds **3** were synthesized according to the literature method [23]. To a suspension of sodium hydride (0.24 g, 10mmol) in dry THF (100mL) was added dropwise triethyl phosphonoacetate (2.34 g, 10mmol) at 0°C under nitrogen atmosphere. The mixture was stirred for 1 h at 0 °C and then the appropriate ketone (6.76mmol) in 15mL THF was added dropwise. After stirring at room temperature for 2 days and then cooled with a water bath, a saturated aqueous ammonium chloride solution (20mL) was added dropwise to the cold mixture. The aqueous phase was extracted with ethyl acetate (3 × 40mL) and the combined organic phase was washed with brine (3 × 30mL), dried over sodium sulphate and concentrated under reduced pressure. The crude residue was purified by column chromatography on silica gel to afford compounds **3** in 70–85% yield.

Fig.2

*2.2.2 General procedure for the preparation of **6***

Compounds **6** were synthesized according to the literature method [14].

*2.2.3 General procedure for the preparation of **7a-g** and **8***

To a 50-mL round-bottomed flask were added **6** (1.00 mmol), an α, β-unsaturated esters **3** (1.20 mmol), potassium carbonate (0.28 g, 2.05 mmol) and dry DMF (10 mL). The mixture was stirred at 50 °C for 8-12 h and then filtered. The filtrate was poured into water (100 mL) and extracted with CH_2Cl_2 (3 × 30 mL). The combined extracts were washed with water, dried over anhydrous $MgSO_4$ and filtered, and the solvent

was removed by rotary evaporation. The crude products were purified by column chromatography to afford compound **7a-g** and **8** in 42-68%.

*2.2.3.1 ethyl 2-acetyl-6-phenylindolizine-7-carboxylate (**7a**).*

Yellow solid (62% yield): mp 110.4-111.6 °C; ^{1}H NMR (300 MHz, $CDCl_3$): δ = 8.10 (s, 1H), 7.85 (d, *J* = 0.9 Hz, 1H), 7.77 (s, 1H), 7.41-7.28 (m, 5H), 7.05 (s, 1H), 4.09 (q, *J* = 7.2 Hz, 2H), 2.56 (s, 3H), 1.03 (t, *J* = 7.2 Hz, 3H); ^{13}C NMR (100 MHz, $CDCl_3$): δ = 194.5, 166.4, 138.0, 131.0, 130.1, 128.6, 128.0, 127.5, 126.8, 125.0, 124.7,122.6, 116.8, 103.9, 61.0, 27.7, 13.7; IR (KBr) ν = 3126, 3062, 2983, 2904, 1737, 1700, 1669, 1627, 1483, 1400, 1273, 1091cm^{-1}; HRMS: *m/z* calcd for $C_{19}H_{18}NO_3$ $[M+H]^+$ 308.1287, found 308.1282.

*2.2.3.2 ethyl 2-acetyl-6-(4-methoxyphenyl)indolizine-7-carboxylate (**7b**).*

Yellow solid (55% yield): mp 182.8-185.7 °C; ^{1}H NMR (300 MHz, $CDCl_3$): δ = 8.09 (s, 1H), 7.83 (d, *J* = 0.9 Hz, 1H), 7.75 (s, 1H), 7.23 (d, *J* = 9.0 Hz, 2H), 7.04 (s, 1H), 6.93 (d, *J* = 9.0 Hz, 2H), 4.12 (q, *J* = 7.2 Hz, 2H), 3.84 (s, 3H), 2.57 (s, 3H), 1.10 (t, *J* = 7.2 Hz, 3H); ^{13}C NMR (100 MHz, $CDCl_3$): δ = 194.5, 166.4, 159.2, 131.0, 130.2, 130.0, 129.7, 126.5, 124.8, 124.6, 122.7, 116.6, 113.5, 103.9, 61.0, 55.3, 27.7, 13.9; IR (KBr) ν = 3127, 3064, 2982, 2902, 1700, 1667, 1627, 1486, 1405, 1270, 1091cm^{-1}; HRMS: *m/z* calcd for $C_{20}H_{20}NO_4$ $[M+H]^+$ 338.1392, found 338.1396.

*2.2.3.3 ethyl 2-acetyl-6-(4-chlorophenyl)indolizine-7-carboxylate(**7c**).*

Yellow solid (68% yield): mp 184.6-185.9 °C; ^{1}H NMR (300 MHz, $CDCl_3$): δ = 8.16 (s, 1H), 7.86 (d, *J* = 0.9 Hz, 1H), 7.75 (s, 1H), 7.37 (d, *J* = 8.4 Hz, 2H), 7.24 (d, *J* = 8.4 Hz, 2H), 7.08 (s, 1H), 4.13 (q, *J* = 7.2 Hz, 2H), 2.58 (s, 3H), 1.11 (t, *J* = 7.2 Hz,

3H); ^{13}C NMR (100 MHz, $CDCl_3$): δ = 194.4, 166.0, 136.5, 133.6, 131.1, 130.3, 130.0, 128.2, 125.8, 125.1, 125.0, 121.9, 116.9, 104.3, 61.1, 27.8, 13.9; IR (KBr) ν = 3128, 3055, 2983, 2913, 1699, 1671, 1628, 1484, 1402, 1279, 1093cm^{-1}cm^{-1}; HRMS: *m/z* calcd for $C_{19}H_{17}ClNO_3$ $[M+H]^+$ 342.0897, found 342.0899.

*2.2.3.4 ethyl 2-acetyl-6-(naphthalen-2-yl)indolizine-7-carboxylate (**7d**).*

Yellow solid (45% yield): mp 124.6-126.8 °C; ^{1}H NMR (300 MHz, $CDCl_3$): δ = 8.28 (s, 1H), 7.88-7.83 (m, 4H), 7.59-7.34 (m, 5H), 7.14 (s, 1H), 3.75 (q, *J* = 7.2 Hz, 2H), 2.58 (s, 3H), 0.54 (t, *J* = 7.2 Hz, 3H); ^{13}C NMR (100 MHz, $CDCl_3$): δ = 194.5, 165.7, 136.1, 133.2, 133.1, 131.4, 130.2, 128.3, 18.1, 126.6, 126.3, 125.8, 125.6, 125.3, 125.2, 124.9, 123.2, 116.9, 104.4, 60.6, 27.8, 13.1; IR (KBr) ν = 3128, 3056, 2977, 2902, 1700, 1677, 1622, 1479, 1398, 1269, 1183, 1078cm^{-1}; HRMS: *m/z* calcd for $C_{23}H_{20}NO_3$ $[M+H]^+$ 358.1443, found 358.1440.

*2.2.3.5 ethyl 2-acetyl-6-(thiophen-2-yl)indolizine-7-carboxylate (**7e**).*

Yellow solid (42% yield): mp 110.8-112.5 °C; ^{1}H NMR (300 MHz, $CDCl_3$): δ = 8.07 (s, 1H), 7.92 (s, 1H), 7.85 (d, *J* = 0.9 Hz, 1H), 7.34 (dd, *J* = 1.2, 4.8 Hz, 1H), 7.07-7.01 (m, 3H), 4.17 (q, *J* = 7.2 Hz, 2H), 2.57 (s, 3H), 1.15 (t, *J* = 7.2 Hz, 3H); ^{13}C NMR (100 MHz, $CDCl_3$): δ = 194.4, 166.0, 138.6, 131.0, 130.3, 127.1, 126.9, 1225.9, 125.7, 124.4,122.9, 119.3, 116.8, 104.2, 61.4, 27.8, 13.8; IR (KBr) ν = 3125, 3075, 2978, 2905, 1704, 1667, 1627, 1482, 1397, 1271, 1086cm^{-1}; HRMS: *m/z* calcd for $C_{17}H_{16}NO_3S$ $[M+H]^+$ 314.0851, found 314.0856.

*2.2.3.6 ethyl 2-benzoyl-6-(4-chlorophenyl)indolizine-7-carboxylate (**7f**).*

Yellow solid (60% yield): mp 97.2-103.7 °C; ^{1}H NMR (300 MHz, $CDCl_3$): δ =

8.19 (s, 1H), 7.94-7.91 (m, 2H), 7.87 (s, 1H), 7.77 (s, 1H), 7.63-7.49 (m, 3H), 7.38 (d, J = 8.4 Hz, 2H), 7.25 (d, J = 8.4 Hz, 2H),7.14 (s, 1H), 4.14 (q, J = 7.2 Hz, 2H), 1.12 (t, J = 7.2 Hz, 3H); ^{13}C NMR (100 MHz, $CDCl_3$): δ = 191.3, 166.0, 139.0, 138.6, 132.2, 130.8, 129.4, 129.0, 128.4, 127.1, 126.9, 125.9, 125.7, 124.4, 122.9, 119.3, 118.6, 61.1, 13.9; IR (KBr) ν = 3115, 3076, 2981, 1708, 1631, 1478, 1394, 1265, 1120cm^{-1}; HRMS: *m/z* calcd for $C_{24}H_{19}ClNO_3$ $[M+H]^+$ 404.1053, found 404.1055.

*2.2.3.7 ethyl 2-benzoyl-6-(thiophen-2-yl)indolizine-7-carboxylate (**7g**).*

Yellow solid (45% yield): mp 131.8-133.4 °C; ^{1}H NMR (300 MHz, $CDCl_3$): δ = 8.10 (s, 1H), 7.94-7.91 (m, 3H), 7.84 (d, J = 0.9 Hz, 1H), 7.63-7.48 (m, 3H), 7.36-7.34 (dd, J = 1.6, 5.1 Hz, 1H), 7.12 (s, 1H), 7.07-7.00 (m, 2H), 4.18 (q, J = 7.2 Hz, 2H), 2.57 (s, 3H), 1.14 (t, J = 7.2 Hz, 3H); ^{13}C NMR (100 MHz, $CDCl_3$): δ = 191.3, 166.0, 139.0, 136.6, 133.6, 132.2, 130.8, 129.4, 130.0, 129.4, 129.0, 128.4, 128.2, 125.8, 125.1, 125.0, 121.9, 118.6, 61.1, 13.9; IR (KBr) ν = 3124, 3054, 2979, 1721, 1641, 1462, 1271, 1086cm^{-1}; HRMS: *m/z* calcd for $C_{22}H_{18}NO_3S$ $[M+H]^+$ 376.1007, found 376.1001.

*2.2.3.8 ethyl 4-(4-acetyl-2-formyl-1H-pyrrol-1-yl)-3-(thiophen-2-yl)but-2-enoate (**8**).*

Yellow solid (65% yield): ^{1}H NMR (300 MHz, $CDCl_3$): δ 9.66 (d, J = 0.9 Hz, 1H), 7.56 (s, 1H), 7.30 (m, 2H), 7.24 (m, 1H), 6.97 (m, 1H), 6.51 (s, 1H), 6.13 (s, 2H), 4.25 (q, J = 7.2 Hz, 2H), 2.37 (s, 3H), 1.34 (t, J = 7.2 Hz, 3H).

2.3. X-ray crystallography

Single crystals of compound **7a** suitable for X-ray diffraction were obtained by slow evaporation of a solution of the solid in ethyl acetate at room temperature for 2

days. A crystal with approximate dimension of 0.28 mm × 0.24 mm × 0.21 mm was mounted on a Bruker Smart Apex II CCD equipped with a graphite monochromated MoKα radiation (λ= 0.71073Å) by using Φ and ω scan modes and the data were collected at 293(2) K. The structure of the crystal was solved by direct methods and refined by full-matrix least-squares techniques implemented in the SHELXTL-97 crystallographic software. The non-hydrogen atoms were refined anisotropic ally. The hydrogen atoms bound to carbon were located by geometrical calculations, with their position and thermal parameters being fixed during the structure refinement. A summary of the crystallographic data and structure refinement details is given in Table 1, and the selected bond lengths and angles are presented in Table 2. The crystal structure and cell structure of **7a** are shown in Figs. 3 and 4, respectively.

Table 1 and Table 2

Fig. 3 and Fig. 4

3. Results and discussion

3.1 Synthesis

The desired indolizines **7** were obtained by the reactions of compounds **6** and the bromoaryl substituted esters **3** in the presence of K_2CO_3. It is noted that the presence of a benzoyl or acetyl substituent of pyrrole did not show any significant influence on the outcome of the reaction but the presence of an aryl substituent on the α, β-unsaturated ester interfered with the reaction because of the electric effect. Increased temperature (50 °C) and extended reaction time (up to 12 h) was required to obtain the desired product compared with the previous report[14]. Additionally, we

obtained the intermediate ethyl 4-(4-acetyl-2-formyl-1*H*-pyrrol-1-yl)-3-(thiophen-2-yl)but-2-enoate **8** under room temperature. On the basis of the above results and our previous work [13-16], we believe that this reaction proceeds by an S_N2 displacement of bromide ion, deprotonation resulting in an ester stabilised anion which facilitates cyclisation and a subsequent dehydration as shown in Fig. 5.

Fig. 5

3.2. Structure characterization

The structures of products **7a-g** were characterized by spectroscopic methods (^{1}H NMR, ^{13}C NMR, IR and HRMS). For example, compound **7a**, obtained as yellow crystals, gave a [M + H]-ion peak at *m/z* 308.1282 in the HRMS, in accord with the molecular formula $C_{19}H_{18}NO_3$. The IR spectra showed the characteristic absorption bands at 3062 (Ar-H), 2983(CH_3), 2904(CH_2), 1700 (C=O), 1669 (C=N), 1627 (C=C), 1273 (C-O-C) and the ^{1}H NMR spectra ($CDCl_3$) revealed five distinct singlets at δ 2.56 (3H, -$COCH_3$), 2.42 (3H, CH_3), 2.47 (3H, CH_3), 7.05 (1H, pyrrole moiety), 7.77 (1H, pyrrole moiety) and 8.10 (1H, pyridine moiety). Moreover, compound **7a** showed peaks at δ 1.03 (t, 3H, *J* = 7.2 Hz), 4.09 (q, 2H, *J* = 7.2 Hz), assigned to the protons of ethoxycarbonyl group. All other signals are consistent with the structure of **7a**.

3.3. Crystal structure

The crystal structure of **7a** is in a triclinic system with a P-1 space group. The indolizine subunit is substantially planar with a dihedral angle of 1.47° between pyrrole and pyridine segments. The dihedral angle between the indolizine ring and

phenyl ring is 55.21°. Selected bond lengths and bond angles are listed in Table 2. The results reveal that the carbon-carbon bond lengths on the molecular skeleton are basically intermediate between typical C-C single (1.54 Å) and C-C double (1.34 Å) bonds. The carbon-nitrogen bond lengths are also intermediate between typical C-N single (1.47 Å) and C=N double (1.27 Å) bonds. This indicates that the π-electrons in the molecule are delocalized.

*3.4. Absorption spectral characteristics of the compounds **7a-g***

For UV-visible absorption measurements, the dye concentration was 1×10^{-5} mol L^{-1}, and the UV-visible absorption spectra of compounds **7a-g** are given in Fig. 6. The absorption data are summarized in Table 3. Several absorption peaks could be observed in the wavelength range from 230 to 420 nm, while almost no absorption was observed beyond 425 nm. It is noted that **7a-g** display very similar absorptions with a strong absorption band at ca. 270 nm, which should originate from the benzene ring and indolizine ring and should be assigned to the π-π* electronic transition. The relatively weak absorption bands between 300 and 420 nm are assigned to the n-π* electronic transition.

The data indicated that the structure of 6-aryl group only slightly affects the absorption bands while 2-acyl group obviously affects the absorption. Compounds **7a**, **7b, 7c** and **7e** demonstrate similar absorption properties, with absorption peaks at 269 nm, 266 nm, 272 nm and 267 nm, respectively. The result reveals that 6-phenyl ring, substituent groups (OCH_3, Cl) on 6-phenyl ring or 6-thiophenyl ring slightly affect the absorption character of these compounds. As the steric hindrance of the 6-aryl ring

increased, the maximum absorption of compound **7d** with the 2-naphthyl ring is blue-shifted to 261nm compared to compound **7a**, which indicates that the conjugated π-system between the 6-aryl ring and indolizine ring decreases due to steric hindrance effect. Comparing with **7c** and **7e** the absorption maxima of compounds **7f** and **7g**, in which a benzoyl group is bonded to the C-2 position of indolizine ring, are red shifted 7 nm and 13 nm, respectively. The difference in absorption spectra is due to the fact that the phenyl group enhances the extent of conjugation in compounds **7f** and **7g**.

Influence of solvent on the absorption behavior was investigated. The absorption spectra of **7a**, as an example, in three different solvents (cyclohexane, dichloromethane and acetonitrile) at a concentration of 1×10^{-5} mol L^{-1} are shown in Fig. 7. It is observed that the absorption spectra change slightly with the increase of solvent polarity although there is a tendency of a shorter λ_{max} in acetonitrile, indicating that there is no charge transfer in the ground state.

Table 3

Fig. 6 and Fig. 7

3.5. Fluorescence spectral characteristics

The emission spectra of compounds **7a-g** in dichloromethane solution (1×10^{-6} mol L^{-1}) are presented in Fig. 8 and the data were summaries in Table 3. They present efficient blue emissions in dilute solution, with maximum emission spectra ranging from 434 to 456 nm. The fluorescence maximum emission bands of **7a-g** are dependent on the groups bonded to indolizine rings. The emission maxima of **7b**, **7c**, **7d** and **7e**, in which -OCH_3Ph, -ClPh, thiophenyl and naphthalenyl are bonded to the

C-6 position of indolizine ring, are red-shifted by 12, 11, 10 and 12 nm, respectively, compared to **7a**. The emission maxima of **7f** and **7g**, in which benzoyl bonded to the C-2 position of indolizine ring, are red-shifted by 9 and 10 nm, respectively, compared to **7c** and **7e**. Those rusults might be attributed to the different conjugation degree and different electronic effects in these compounds.

Fig. 8

It can also be found that their intensity of fluorescence differed from each other. The fluorescence intensity of compounds **7e-g** are extremely weak compared with other compounds, which may be due to the interaction of molecules leading to the quenching of fluorescence at the measured concentration of 1×10^{-6} mol L^{-1}. For compound **7g**, the Donor-Acceptor structure character resulting from the electrondonating thiophenyl group and electron-withdrawing benzoyl and ester groups is in favor of dipole-dipole interactions between molecules.

The Stoke's shifts range from 165 to 183 nm, indicating the existence of molecular conformation deviation between the ground state and the exited state. Fluorescence quantum yields (Φ_F) in CH_2Cl_2 were determined by a comparative method, using quinine sulfate as standard. The highest Φ_F value of 0.39 is observed for **7a**, which is higher than that of other compounds. The fluorescence quantum yields of the other compounds are in the range of 0.02-0.27. This difference might be due to the change of the electronic push-pull substitution of the conjugated part in the molecules.

The solvent effects on the fluorescence characteristics of these compounds were

investigated in cyclohexane, CH_2Cl_2 and CH_3CN at the concentration of 1×10^{-6} mol L^{-1}. For compound **7d** in Fig. 9, the emission wavelengths are red shifted with the increase of solvent polarity from 435 nm in cyclohexane to 444 nm in CH_2Cl_2 and 449 nm in CH_3CN. Due to the interaction between fluorescent molecules and solvent, the fluorescence is enhanced with the decrease of solvent polarity.

Fig. 9

4. Conclusion

This paper describes the use of a novel tandem reaction to prepare indolizine derivatives under mild conditions in moderate to good yields. The structures of compounds obtained were determined by IR, ^{1}H NMR, ^{13}C NMR, and HRMS spectra, and the spatial structure of compound **7a** was confirmed by X-ray crystallography. Absorption and fluorescence spectral characteristics of the compounds were investigated. Compounds **7f-g** show red-shifted absorption peaks compared to the corresponding absorption of **7a-e**, due to their extended conjugation. These compounds exhibited blue fluorescence (434-456 nm) in dilute solutions and showed acceptable quantum yields of fluorescence in dichloromethane, with the highest Φ_F value of 0.39 for compound **7a**. It can be concluded that the absorption and fluorescence characteristics of compounds **7a-g** show a significant dependence on the structure of 2-acyl group in the C-2 position of indolizine but slightly on 6-aryl group. These small molecules have potential bioactivities and their anticancer activities are currently under investigation.

5. Supplementary materials

CCDC 903100 contains the supplementary crystallographic data for this paper. These data can be obtained free of charge via www.ccdc.cam.ac.uk/data_request/cif, by emailing data_request@ccdc.cam.ac.uk, or by contacting The Cambridge Crystallographic Data Centre, 12, Union Road, Cambridge CB21EZ, UK; fax: t44 1223 336033.

Acknowledgement

We thank the Science and Technology Development Project of Shandong Province (2012GSF11812), the Natural Science Foundation of Shandong Province (ZR2012BL04 and ZR2013BM020) and the Natural Science Foundation of Taishan Medical University (2013GCC02) for financial support.

References

[1] Gubin J, Vogelaer H, Inion H, Houben C, Lucchetti J, Mahaux J, Rosseels G, Peiren M, Clinet M, Polster P, Chatelain P. Novel heterocyclic analogues of the new potent class of calcium entry blockers: 1-[[4-(aminoalkoxy)phenyl]sulfonyl] indolizines. J Med Chem 1993; 36: 1425-33.

[2] Harrell WB, Doerge RF. Mannich bases from 2-phenylindolizines. I. 3-Alkyl-1-dialkylaminomethyl derivatives. J Pharm Sci 1967; 56: 225-8.

[3] Bermudez J, Fake CS, Joiner GF, Joiner KA, King FD, Miner WD, Sanger GJ. 5-Hydroxytryptamine (5-HT3) receptor antagonists. 1. Indazole and indolizine-3-carboxylic acid derivatives. J Med Chem 1990; 33: 1924-9.

[4] Chai W, Breitenbucher JG, Kwok A, Li X, Wong V, Carruthers NI, Lovenberg TW, Mazur C, Wilson SJ, Axe FU, Jones TK. Non-imidazole heterocyclic histamine

H3 receptor antagonists. Bioorg Med Chem Lett 2003; 13: 1767-70.

[5] Gundersen LL, Charnock C, Negussie AH, Rise F, Teklu S. Synthesis of indolizine derivatives with selective antibacterial activity against Mycobacterium tuberculosis. Eur J Pharm Sci 2007; 30: 26-35.

[6] Hagishita S, Yamada M, Shirahase K, Okada T, Murakami Y, Ito Y, Matsuura T, Wada M, Kato T, Ueno M, Chikazawa Y, Yamada K, Ono T, Teshirogi I, Ohtani M. Potent inhibitors of secretory phospholipase A2: synthesis and inhibitory activities of indolizine and indene derivatives. J Med Chem 1996; 39: 3636-58.

[7] Marder SR, Stucky GD, Sohn JE. Materials for Nonlinear Optics. ACS symposium series, vol. 455. Washington, DC: ACS; 1991.

[8] Surpateanu GG, Becuwe M, Lungu NC, Dron PI, Fourmentin S, Landy D, Surpateanu G. Photochemical behaviour upon the inclusion for some volatile organic compounds in new fluorescent indolizine β-cyclodextrin sensors. J Photoch Photobio A 2007; 185: 312-20.

[9] Delattre F, Oisel P, Surpateanu G, Cazier F, Blach P. 1-(4-nitrophenoxycarbonyl)-7-pyridin-4-yl indolizine: a new versatile fluorescent building block. Application to the synthesis of a series of fluorescent beta-cyclodextrins. Tetrahedron 2005; 61: 3939-45.

[10] Sonnenschein H, Henrich G, Resch-Genger V, Schulz B. Fluorescence and UV/Vis spectroscopic behaviour of novel biindolizines. Dyes Pigm 2000; 46: 23-7.

[11] Saeva FD, Luss HR. Novel synthesis of the 2,3-benzindolizine ring system.

Mechanism of formation, redox, electronic absorption, and fluorescence behavior. J Org Chem 1988; 53: 1804-6.

[12] Ghosh BC, Deb N, Becuwe M, Fourmentin S, Mukherjee AK. Excited state proton transfer assisted fluorescence resonance energy transfer in an inclusion complex of a β-CD derivative. J Photoch Photobio A 2012; 238: 29-34.

[13] Ge YQ, Jia J, Li Y, Yin L, Wang JW. A novel and efficient approach to pyrazolo[1,5-*a*]pyridine derivatives via one-pot tandem reaction. Heterocycles 2009; 78: 197-206.

[14] Ge YQ, Jia J, Yang H, Zhao GL, Zhan FX, Wang JW. A facile approach to indolizines via tandem reaction. Heterocycles 2009; 78: 725-36.

[15] Jia J, Ge YQ, Tao XT, Wang JW. Facile synthesis of imidazo[1,2-*a*]pyridines via tandem reaction. Heterocycles 2010; 81: 185-94.

[16] Ge YQ, Jia J, Yang H, Tao XT, Wang JW. The synthesis, characterization and optical properties of novel pyrido[1,2-a]benzimidazole derivatives. Dyes Pigm 2011; 88(3):344-9.

[17] Ge YQ, Hao BQ, Duan GY, Wang JW. The synthesis, characterization and optical properties of novel 1,3,4-oxadiazole-containing imidazo[1,5-a]pyridine derivatives. J Lumin 2011; 131(5): 1070-6.

[18] Yang H, Ge YQ, Jia J, Wang JW. Synthesis and optical properties of novel pyrido[1,2-a]benzimidazole-containing 1,3,4-oxadiazole derivatives. J Lumin 2011; 131(4):749-55

[19] Ge YQ, Wang T, Duan GY, Dong LH, Cao XQ, Wang JW. Synthesis,

Characterization, Optical Properties and Theoretical Studies of Novel Substituted Imidazo[1,5-a]pyridinyl 1,3,4-Oxadiazole Derivatives. J Fluoresc 2012; 22: 1531-8.

[20] Cao XQ, Lin XH, Zhu Y, Ge YQ. The optical properties, synthesis and characterization of novel 5-aryl-3-benzimidazolyl-1-phenyl-pyrazoline derivatives. Spectrochim Acta Part A 2012; 98: 76-80.

[21] Ge YQ, Jia J, Wang T, Sun HW, Duan GY, Wang JW. The synthesis, characterization and optical properties of novel 5-(3-aryl-1H-pyrazol-5-yl)-2-(3-butyl-1-chloroimidazo[1,5-a]pyridin-7-yl)-1,3,4-oxadiazole, Spectrochim Acta Part A, 2014; 123: 336-41.

[22] Ge YQ, Li FR, Zhang YJ, Bi YS, Cao XQ, Duan GY, Wang JW, Liu ZL. Synthesis, crystal structure, optical properties and antibacterial evaluation of novel imidazo[1, 5-a]pyridine derivatives bearing a hydrazone moiety, Luminescence, 2014, DOI: 10.1002/bio.2547.

[23] Deng J, Duan ZC, Huang JD, Hu XP, Wang DY, Yu SB, Xu XF, Zheng Z. Rh-catalyzed asymmetric hydrogenation of g-phthalimido-substituted α, β-unsaturated carboxylic acid esters: an efficient enantioselective synthesis of β-aryl-γ-amino acids. Org Lett 2007; 9: 4825-8.

Figure Captions:

Table 1 Crystal data and structure refinement for **7a**

Empirical formula	$C_{18}H_{15}NO_3$
Formula weight	293.31
Temperature	293(2) K
Wavelength	0.71073 Å
Crystal system, space group	Triclinic, P-1
Unit cell dimensions	a = 7.685(8) Å α= 74.847(16) °
	b = 8.207(8) Å β = 80.330(19) °
	c = 15.319(15) Å γ = 65.234(15) °
Volume	844.9(15) A^3
Z	2
Calculated density	1.153 Mg/m^3
Absorption coefficient	0.079 mm^{-1}
F(000)	308
Crystal size	0.28 × 0.24 × 0.21 mm
θ range for data collection	1.38-25.05°
Limiting indices	$-6 \le h \le 9$, $-9 \le k \le 9$, $-13 \le l \le 18$
Reflections collected / unique	4238 / 2913 [R(int) = 0.0556]
Completeness to θ = 25.05°	97.6 %
Absorption correction	Semi-empirical from equivalents
Max. and min. transmission	0.9836 and 0.9782
Refinement method	Full-matrix least-squares on F^2
Data / restraints / parameters	2913 / 21 / 204
Goodness-of-fit on F^2	1.027
Final R indices [$I > 2\sigma(I)$]	R_1 = 0.0668, wR_2 = 0.1811
R indices (all data)	R_1 = 0.1119, wR_2 = 0.2135
Largest diff. peak and hole	0.381 and -0.407 e. $Å^{-3}$

Table 2 Selected bond lengths and angles for **7a**

bond lengths							
N(2)-C(4)	1.363(4)	N(2)-C(5)	1.376(4)	N(2)-C(9)	1.416(4)	C(10)-C(3)	1.429(5)
C(6)-C(7)	1.465(4)	C(4)-C(3)	1.382(5)	C(8)-C(7)	1.360(5)	C(8)-C(9)	1.407(5)
C(9)-C(10)	1.373(5)	C(6)-C(5)	1.359(5)				
bond angles							
C(4)-N(2)-C(5)		129.4(3)		C(14)-C(13)-C(18)		118.2(3)	
C(4)-N(2)-C(9)		108.7(3)		C(14)-C(13)-C(6)		120.5(3)	
C(5)-N(2)-C(9)		121.8(3)		C(18)-C(13)-C(6)		121.4(3)	
C(7)-C(8)-C(9)		121.6(3)		C(9)-C(10)-C(3)		107.4(3)	
C(10)-C(9)-C(8)		135.5(3)		C(4)-C(3)-C(10)		107.6(3)	
C(10)-C(9)-N(2)		107.6(3)		C(4)-C(3)-C(2)		126.6(3)	
C(8)-C(9)-N(2)		116.9(3)		C(10)-C(3)-C(2)		125.7(3)	
C(5)-C(6)-C(7)		117.4(3)		O(3)-C(2)-C(3)		121.1(3)	
C(5)-C(6)-C(13)		119.1(3)		O(3)-C(2)-C(1)		121.1(4)	
C(7)-C(6)-C(13)		123.3(3)		C(3)-C(2)-C(1)		117.8(3)	
C(6)-C(5)-N(2)		121.8(3)		C(17)-C(18)-C(13)		120.9(4)	
C(8)-C(7)-C(6)		120.4(3)		C(15)-C(14)-C(13)		120.7(4)	
C(8)-C(7)-C(11)		116.7(3)		C(18)-C(17)-C(16)		120.0(4)	
C(6)-C(7)-C(11)		122.9(3)		C(14)-C(15)-C(16)		121.1(4)	
N(2)-C(4)-C(3)		108.6(3)		C(15)-C(16)-C(17)		119.1(4)	

Table 3 The optical characteristics of the compounds **7a-g** in dichloromethane.

Compounds	λ_{max} (nm)	λ_{ex} (nm)	ε_{max} (L mol^{-1} cm^{-1})	F_{max} (nm)	Stokes shift (nm)	Φ_F
7a	269	400	58500	434	165	0.39
7b	266	400	43700	446	180	0.21
7c	272	400	68400	445	173	0.27
7d	261	400	71800	444	183	0.14
7e	267	400	73200	446	179	0.040
7f	279	400	94900	454	175	0.043
7g	280	400	70300	456	176	0.019

Fig.1 Charge distribution within indolizine moiety

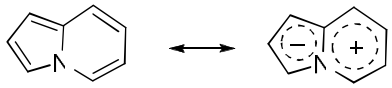

Fig.2 Synthetic routes of **7a-g**

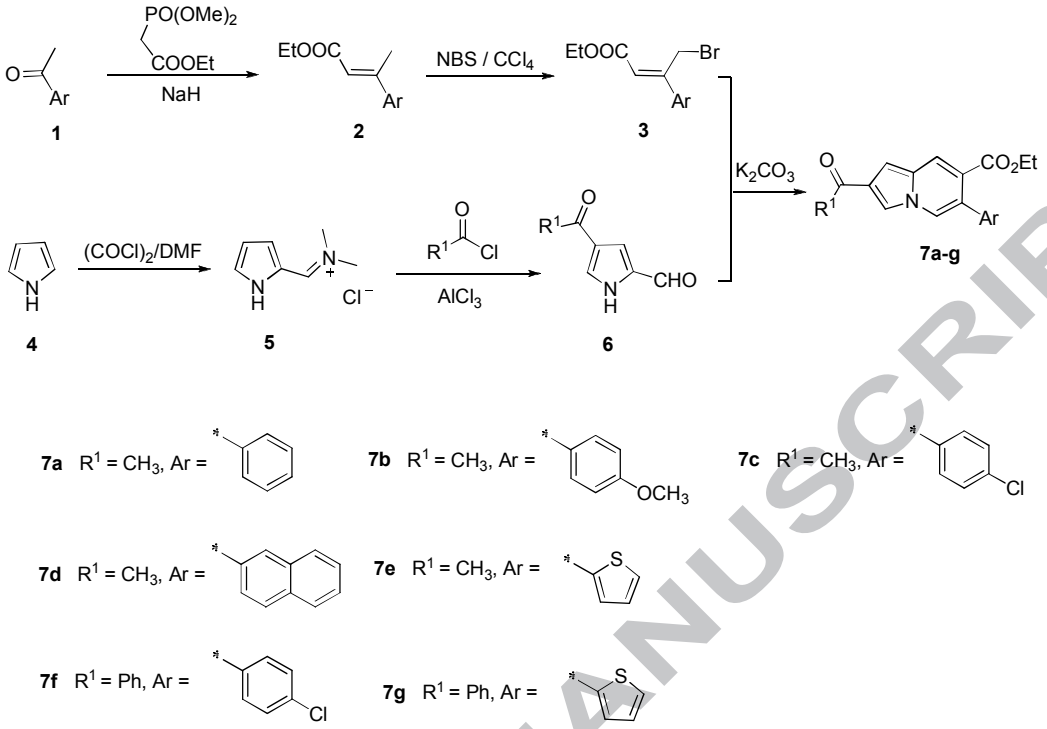

7a $R^1 = CH_3$, Ar =

7b $R^1 = CH_3$, Ar =

7c $R^1 = CH_3$, Ar =

7d $R^1 = CH_3$, Ar =

7e $R^1 = CH_3$, Ar =

7f R^1 = Ph, Ar =

7g R^1 = Ph, Ar =

Fig.2 Synthetic routes of **7a-g**

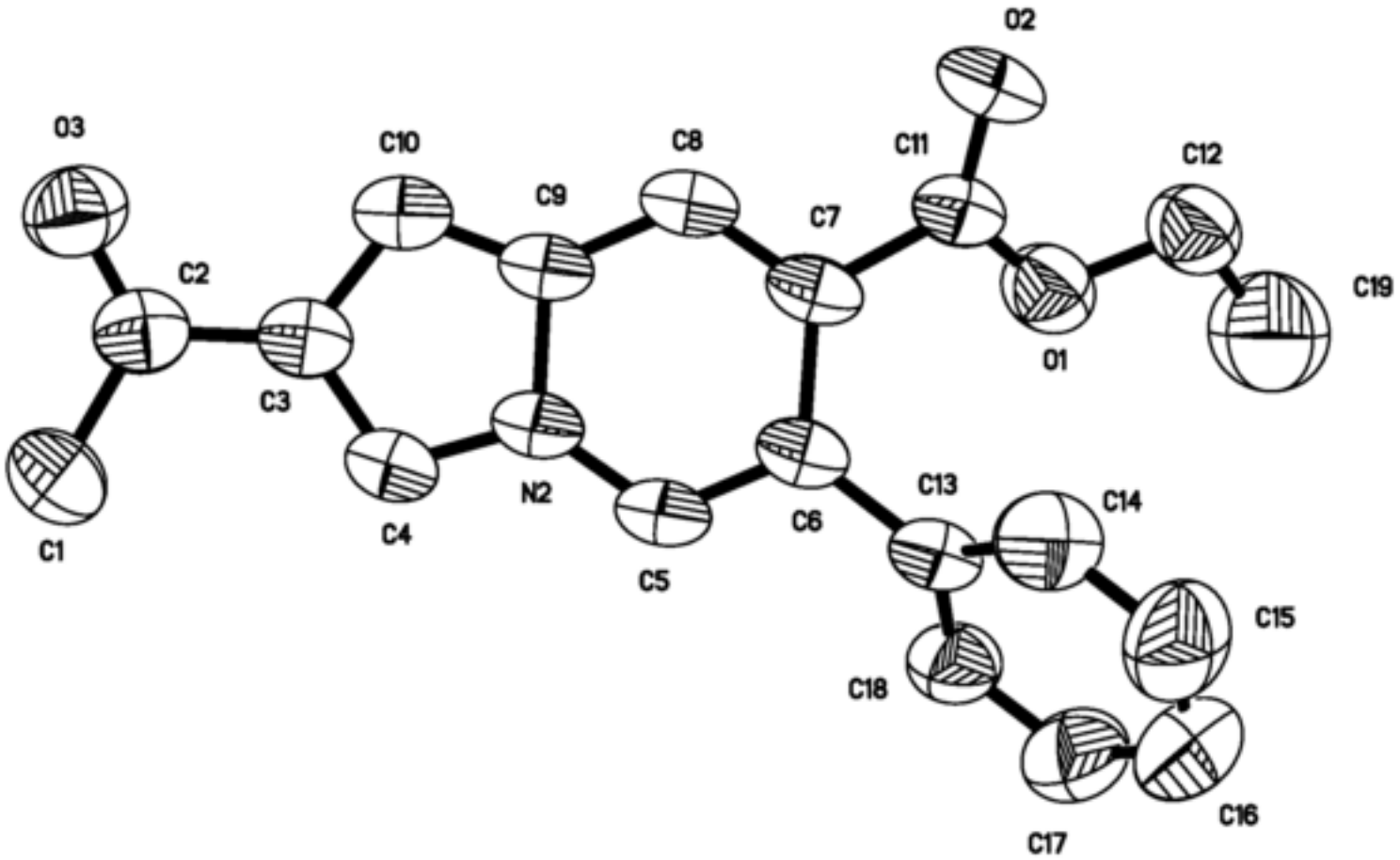

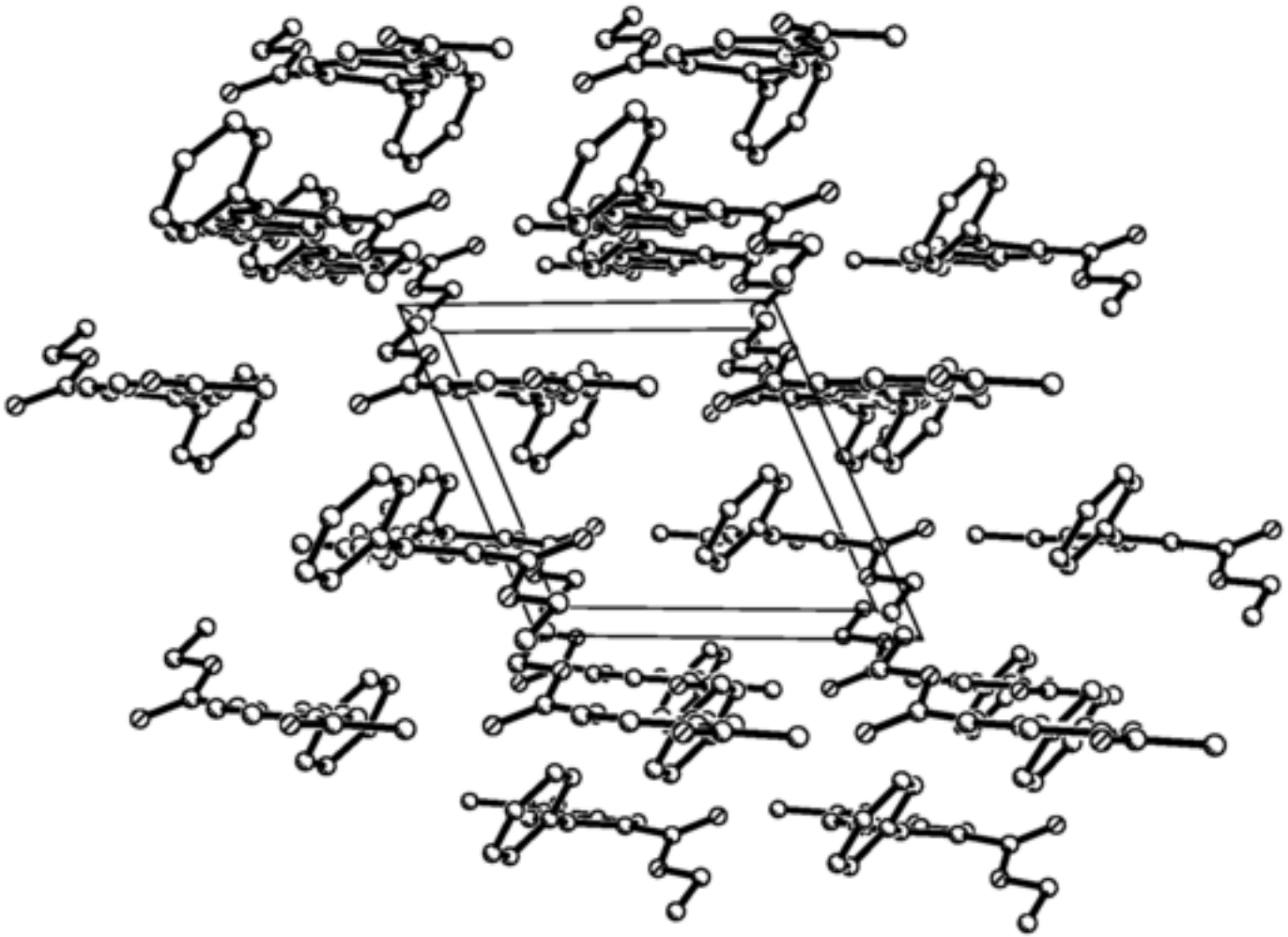

Fig.5 The mechanism of the tandem reaction

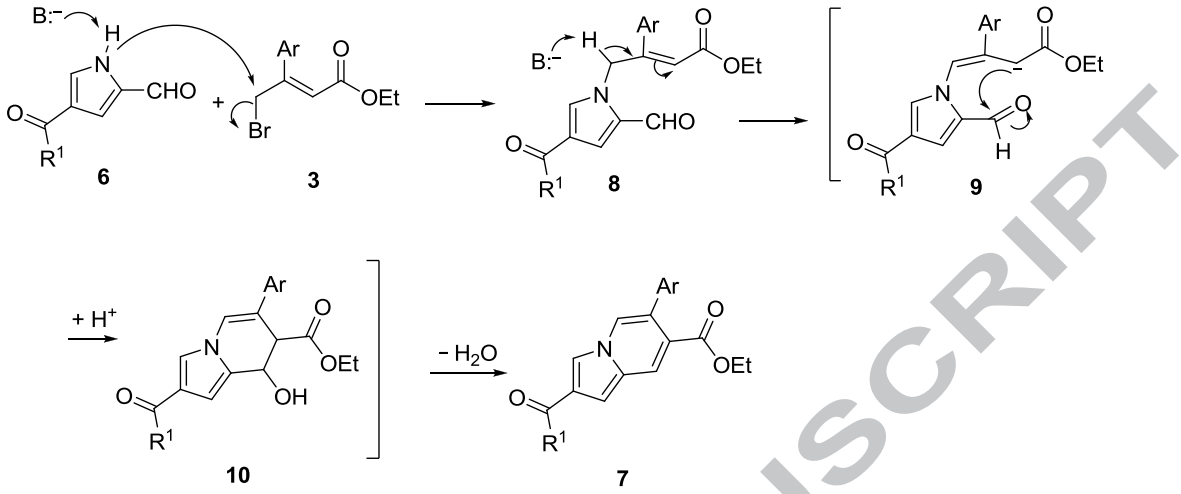

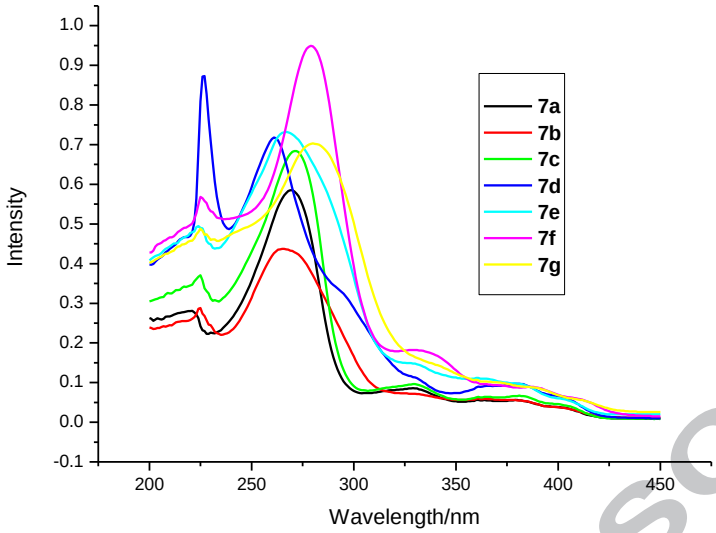

Fig. 6. The UV-vis spectra of the compounds **7a-g** in dichloromethane.

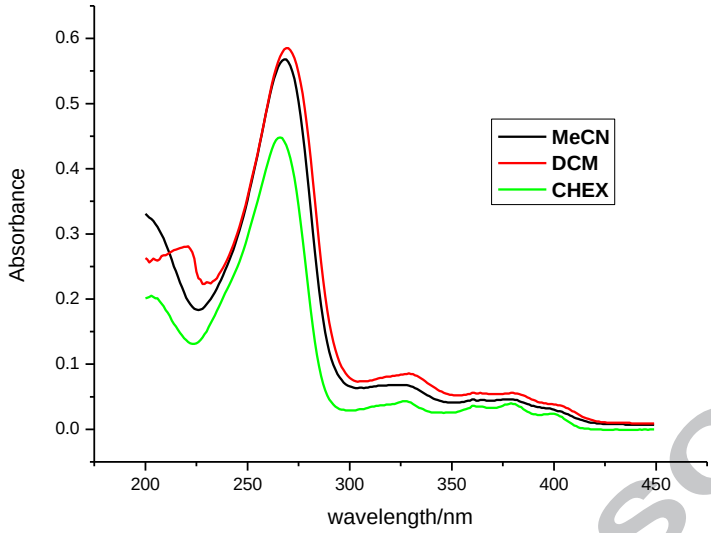

Fig. 7 UV-vis absorption spectrum of compound **7a** in different solvents

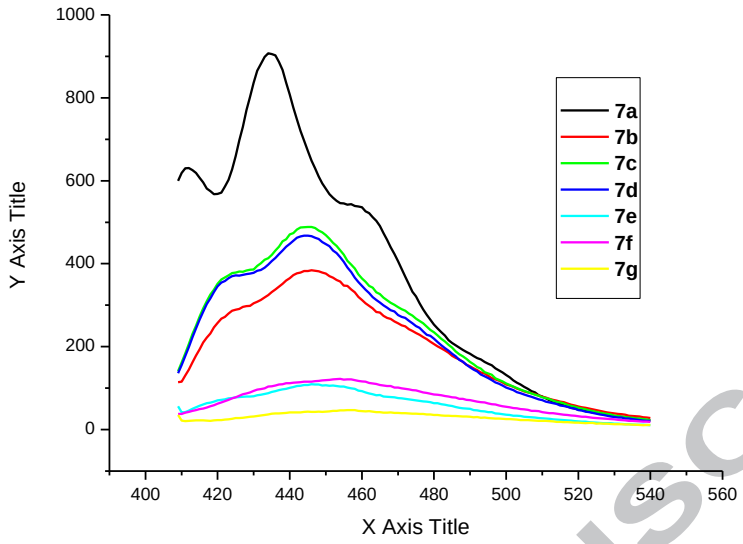

Fig. 8 The Fluorescence spectra of the compounds **7a-g** in dichloromethane.

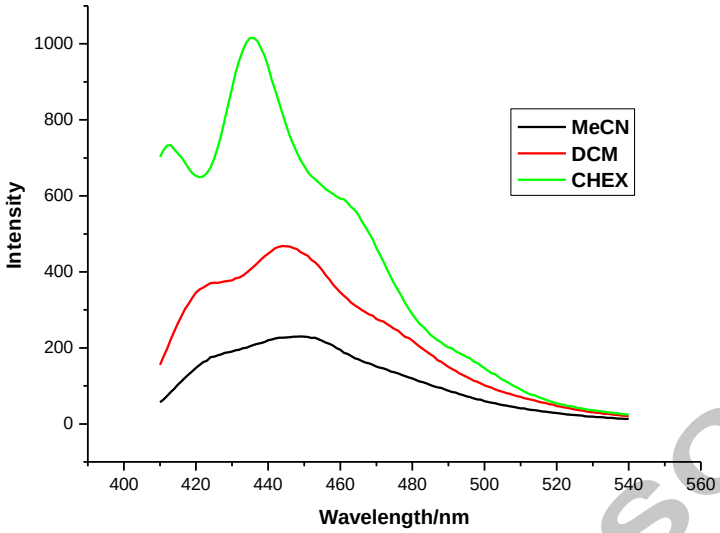

Fig. 9 The fluorescence spectra of compound **7d** in different solvents

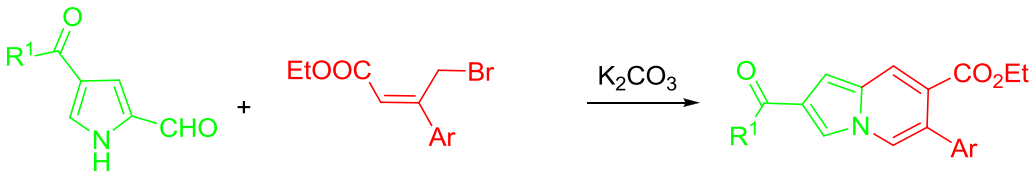

Highlights

♦ Novel indolizine derivatives were prepared by tandem reaction and fully characterized.

♦ UV-vis absorption and fluorescence spectroscopy of all compounds were measured.

♦ Influence of solvent and substituent on UV-vis absorption and fluorescence spectroscopy was examined.